JACS
JOURNAL OF THE AMERICAN CHEMICAL SOCIETY

Article

pubs.acs.org/JACS

Probing Protein Conformation in Cells by EPR Distance Measurements using Gd^{3+} Spin Labeling

Andrea Martorana,[†] Giuliano Bellapadrona,[‡] Akiva Feintuch,[†] Enza Di Gregorio,[§] Silvio Aime,[§] and Daniella Goldfarb*,[†]

[†]Department of Chemical Physics and [‡]Department of Materials and Interfaces, Weizmann Institute of Science, Rehovot, Israel 7610001

[§]Department of Molecular Biotechnologies and Health Sciences, University of Torino, Torino, Italy 10100

Supporting Information

ABSTRACT: Protein structure investigations are usually carried out *in vitro* under conditions far from their native environment in the cell. Differences between *in-cell* and *in vitro* structures of proteins can be generated by crowding effects, local pH changes, specific and nonspecific protein and ligand binding events, and chemical modifications. Double electron–electron resonance (DEER), in conjunction with site-directed spin-labeling, has emerged in the past decade as a powerful technique for exploring protein conformations in frozen solutions. The major challenges facing the application of this methodology to *in-cell* measurements are the instabilities of the standard nitroxide spin labels in the cell environment and the limited sensitivity at conventional X-band frequencies. We present a new approach for *in-cell* DEER distance measurement in human cells, based on the use of: (i) reduction resistant Gd^{3+} chelates as spin labels, (ii) high frequency (94.9 GHz) for sensitivity enhancement, and (iii) hypo-osmotic shock for efficient delivery of the labeled protein into the cell. The proof of concept is demonstrated on doubly labeled ubiquitin in HeLa cells.

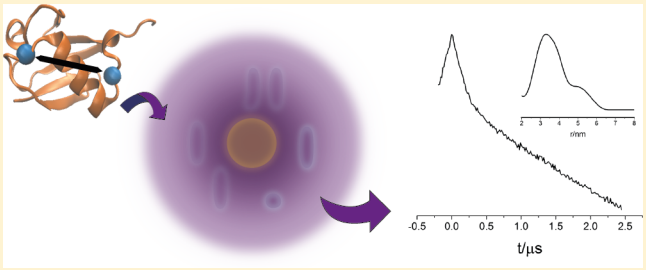

INTRODUCTION

The folding and activity of a protein are strongly influenced by its immediate physicochemical environment. Atomic level structural and dynamic studies of proteins have succeeded to elucidate structures and functions of proteins, thus producing valuable information on proteins, their complexes with substrates, and protein–protein interactions. Such studies are usually carried out under *in vitro* conditions that are often dictated by the method applied. The next level of understanding protein structure and function requires considering the natural cellular environment of the proteins, where parameters such as cytoplasmic crowding, limited protein dynamics, subcellular localization, interaction with other cellular components, and cellular responses may affect the protein structure and dynamics. Accordingly, considerable efforts are currently being devoted to developing methods that probe protein structure and dynamics inside living cells.

Förster's resonance energy transfer (FRET) is a highly sensitive method (single molecule level) that can provide distance between two chromophores on the nanometer-scale in a solution at room temperature. It is excellent for detecting and monitoring the dynamics of conformational changes but it encounters difficulties in measuring with good accuracy distances due to caveats such as the size of the fluorophore labels, dependence on angular orientations of the fluorophores, and background signals due to nonspecific FRET.[1] *In-cell* FRET usually relies on fusion with florescent proteins, and the distance estimated from FRET is between the large protein labels.[2,3] The large size prevents atomic level structural studies[4] but rather allows detecting the presence of interactions. For example, *in-cell* FRET has been used to detect conformational changes in macromolecules,[5] tracking complex formation,[6,7] and analyzing chromatin compaction.[8]

Over the past decade, nuclear magnetic resonance (NMR) spectroscopy has played a major role in providing a look into biomolecular structure in numerous cell types.[9] NMR requires labeling the proteins with stable isotopes such as ^{13}C, ^{15}N, or ^{19}F in order to distinguish the protein under study from the complex intracellular environment background. ^{13}C and ^{15}N enriched proteins can be generated *in situ* in prokaryotic cells by designing their overexpression under isotopically enriched growth conditions. In eukaryotic cells the isotopically enriched (^{13}C, ^{15}N), or labeled protein (^{19}F), have to be delivered into the cells while the labeling is generally carried out *in vitro*. Microinjection into *Xenopus laevis* oocytes,[10] electroporation, use of pore-forming toxins,[11] and cell penetrating peptides (CPP) have been exploited to introduce labeled proteins into cells with the aim of studying protein dynamics,[12] folding processes,[13] protein maturation,[14] and protein–protein interactions.[15] The drawbacks of *in-cell* NMR are related to the inherent low sensitivity of the technique that require large

Received: August 3, 2014
Published: August 28, 2014

   dx.doi.org/10.1021/ja5079392 | J. Am. Chem. Soc. 2014, 136, 13458–13465

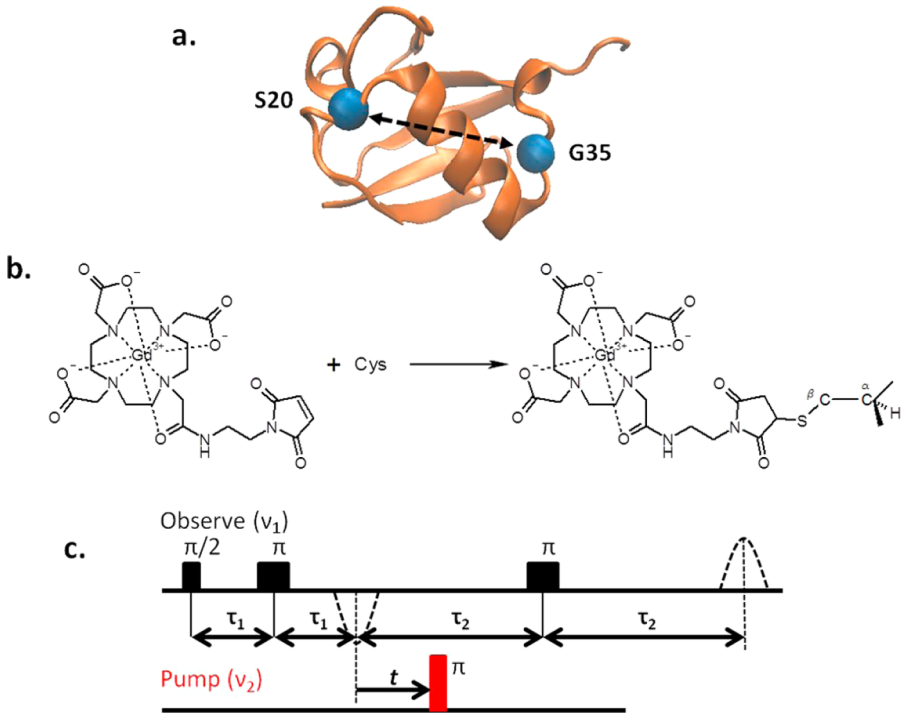

Figure 1. (a) Ribbon structure of the ubiquitin (PDB code 1UBQ). Ser20 and Gly35 were substituted with cysteines and labeled with Gd^{3+}-DOTA-M. (b) Labeling reaction of Gd^{3+}-DOTA-M with cysteine residues. (c) The four pulse DEER sequence.[17]

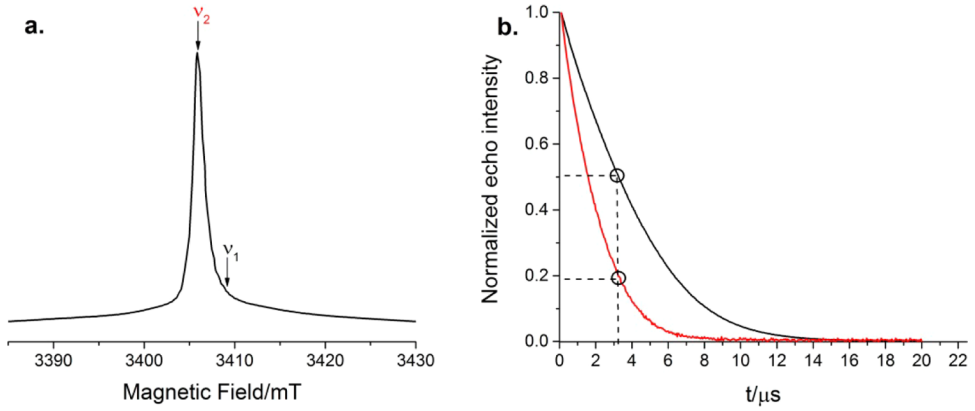

Figure 2. (A) W-band ED EPR spectrum of *in vitro* reference S20C/G35C-Gd^{3+}-DOTA-M solution at 10 K. The position of the pump (ν_2) and observer (ν_1) frequencies are shown. (b) Two pulse-echo decay of the *in-cell* (red) and *in vitro* (black) samples at the observer frequencies. The open circles correspond to the τ_2 value of the DEER experiment.

sample volumes (~200 μL, of cell suspension) of 20−200 μM *in-cell* concentration, and the limitation to small, fast-tumbling proteins. The low sensitivity implies extended measurements that require keeping the cell viable for a long time, and the high concentrations result in *in-cell* conditions that may deviate significantly from physiological conditions.

In recent years, pulsed electron−electron double resonance (PELDOR or DEER) has emerged as another technique that can provide atomic level structural information on biomolecules through distance measurements between spin labels. It is carried out at low temperatures on frozen solutions, and therefore the dynamic information is lost, but it may be recovered from the width of the distance distribution.[16,17] Due to its inherently higher absolute sensitivity, compared to NMR, DEER can potentially develop into an efficient method for *in-cell* structural studies. While the *in-cell* environment is characterized by thousands of cellular components that can interfere with the biomolecule under study, DEER is sensitive only to paramagnetic systems, and therefore background interference is expected to be negligible. Indeed, a few *in-cell* DEER proof of principle demonstrations have recently been reported.[18−21] These highlighted two major challenges. The first one is that the commonly used nitroxide spin label is reduced and converted into a diamagnetic hydroxylamine in a cellular environment (half-life of approximately 50 min).[18] This limits the delivery method to instantaneous microinjection (followed by immediate freezing) to oocytes, which considerably narrows the scope of the approach and prevents time evolution explorations. Another major difficulty is the limited sensitivity, as the measurements were carried out at standard X-band (~9.5 GHz) frequencies. These measurements required ~50 oocytes per sample with an *in-cell* concentration of ~200 μM;[18] orders of magnitude above proteins' physiological concentrations. Therefore, for DEER to become a viable *in-*

dx.doi.org/10.1021/ja5079392 | J. Am. Chem. Soc. 2014, 136, 13458−13465

cell structure determination method it is essential to (i) design new spin labels that are stable under *in-cell* conditions and accommodate a variety of delivery methods into different cell lines and (ii) increase the sensitivity in order to access concentrations closer to the physiological ones.

Here we report the results of a new approach for *in-cell* DEER distance measurement based on the use of a new family of spin labels, Gd^{3+} chelates, high-frequency (W-band, 94.9 GHz) DEER measurements, and the use of human cells. In brief, a mutant of human ubiquitin bearing two cysteines at Ser20 and Gly35 (see Figure 1a), denoted hereafter as S20C/G35C, was doubly labeled with Gd^{3+}-DOTA maleimide (Gd^{3+}-DOTA-M)[22] (Figure 1b) and introduced into human cervical cancer (HeLa) cells through an osmotic shock.[23,24] Intramolecular distances were determined by four-pulse DEER sequence[17] (Figure 1c). W-band Gd^{3+}–Gd^{3+} distance measurements have already been shown to enjoy a gain in high absolute sensitivity *in vitro*, where sample requirements are 2–3 μL of a ~25–50 μM solution (total 0.05–0.15 nmols protein).[25,26] We show that DEER measurements of ubiquitin within HeLa cells at an estimated *in-cell* concentration of ~20 μM are feasible and we observed no significant differences between the *in vitro* and the *in-cell* distance distribution.

RESULTS

The EPR Spectrum and Echo Decay Rates. The echo-detected (ED) EPR spectrum of S20C/G35C-Gd^{3+}-DOTA-M *in vitro* (25 μM) and *in-cell* (see Figure 2a) is the same, but significant differences are observed in the echo decay rate as shown in Figure 2b. The echo decay is a very important feature of DEER measurements because it affects the sensitivity and determines the longest distance that can be accessed.[27] A common way of extending the echo decay time in *in vitro* measurements is to use deuterated solvent,[28] as was also done here. The intracellular compartment contains mostly water, and this makes the *in-cell* echo decay much faster than *in vitro*, considerably reducing the SNR. Increasing the *in-cell* echo decay rate by using deuterated cellular media is one possible solution, but effects on biochemical functions of the cells in D_2O-containing media should be taken into account. At concentrations (v/v) below 20%, D_2O is considered an antiproliferative agent, but it has been shown that growing cells using high volumes of D_2O up to 90% can seriously damage cell membranes within 48 h.[29] For this reason, we used 90% deuterated buffer only for the last washing. To assess the viability of the cells after this treatment, they were seeded again, and no change in the cellular viability was observed up to 24 h. This procedure increased the decay time of the *in-cell* samples by 60%. In terms of DEER experiments, this represents a considerable improvement as it increased τ_2 from 1.75 to 3.2 μs. Figure 2b (red line) shows 20% of the echo intensity for τ_2 = 3.2 μs (compared to 50% for the *in vitro* sample). The echo decay is still faster than *in vitro* because of the presence of surrounding biomolecules (that bear many protons) and the high local concentration, as evident from the strong background decay in the DEER data, as discussed later.

DEER Measurements. Figure 3 presents a comparison of DEER results for S20C/G35C-Gd^{3+}-DOTA-M *in vitro* (black line) and *in-cell* (red line). In Figure 3a, the original DEER data and the background fit are shown. The data after background removal are presented in Figure 3b, and the derived distance distribution is depicted in Figure 3c. The *in vitro* DEER trace shows a modulation depth, λ, of 4.7% with an SNR of 43 in

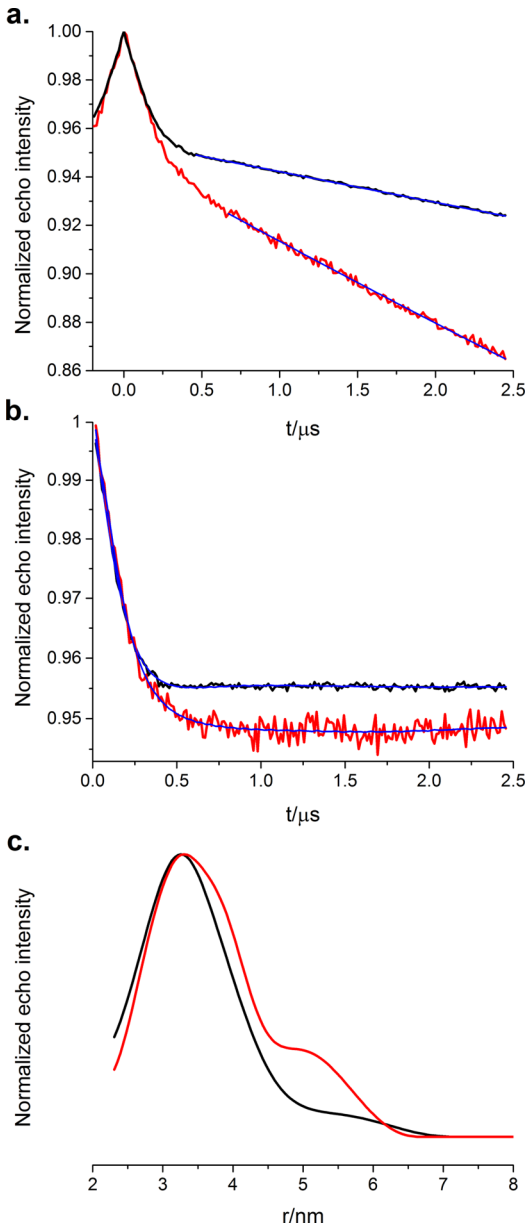

Figure 3. W-band DEER results of S20C/G35C-Gd^{3+}-DOTA-M *in vitro* and *in-cell*. (a) Experimental DEER trace and background fit (blue) of *in vitro* (black, 25 μM) and *in-cell* (red) samples; (b) background corrected DEER traces; and (c) distance distribution obtained using DeerAnalysis.[30]

only 3 h of acquisition time. On the other hand, *in-cell* DEER trace shows a SNR of 11 after 18 h of acquisition and a comparable λ. The distance distribution obtained from both samples is similar: it has a maximum around 3.2 nm and a width of about 1.5 nm (at half-maximum). We note that the background decay is larger in the *in-cell* sample, and this will be discussed later.

In order to demonstrate the stability of Gd^{3+}-DOTA-M in the cell, a DEER experiment was recorded 5 h after osmotic shock (see Supporting Information). After swelling, the cells were resuspended in complete growth media and plated in culture dishes previously treated with fibronectin from bovine plasma. After 5 h, HeLa cells adherent to the culture dish were recovered and loaded into an EPR quartz capillary. The DEER trace obtained was similar to that recorded immediately after

dx.doi.org/10.1021/ja5079392 | J. Am. Chem. Soc. 2014, 136, 13458–13465

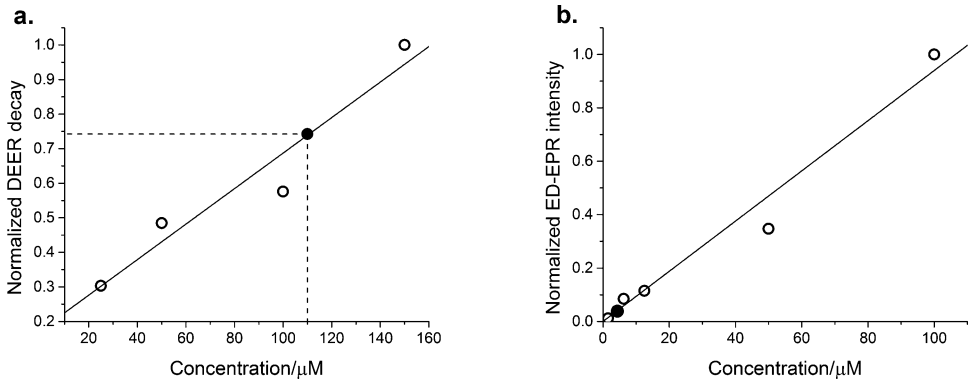

Figure 4. (a) Calibration curve obtained using the background decay slope of the DEER experiment on a series of S20C/G35C-Gd^{3+}-DOTA-M in D_2O/d_8-glycerol solutions (7/3) (solid symbols). (b) Calibration curve obtained from ED EPR spectra of the same series of samples as in (a). All data were normalized to the point with the highest value. The data point of the *in-cell* sample is shown as a full black symbol.

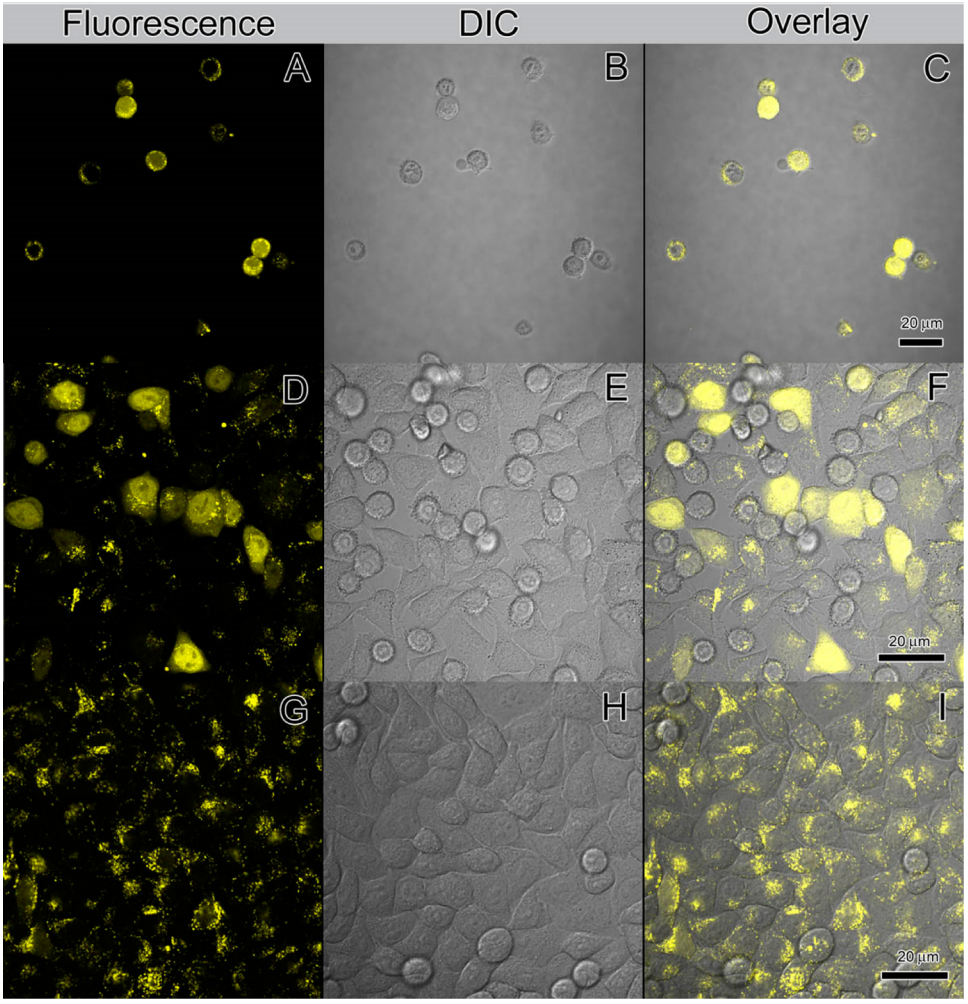

Figure 5. Confocal fluorescence images (left column, A, D, G), differential interference contrast images (central column, B, E, H) and overlays (right column, C, F, I) of HeLa cells at different stages after uptake of S20C/G35C-ATTO488-M. Images were taken immediately after osmotic shock in phosphate saline buffer (A–C), 3 h after recovery (D–F) and 18 h after recovery (G–I). Scale bar is 20 μm.

osmotic shock, confirming the stability of Gd^{3+}-DOTA-M spin label under reductive conditions of cellular cytoplasm.

The next step is to estimate the *in-cell* concentration of the protein. The DEER time domain signal is the product of two different contributions, namely the intermolecular (V_{inter}) and intramolecular (V_{intra}) dipolar interactions. V_{intra} yields information about intramolecular spin–spin distances and V_{inter} gives information about the local spin concentration and the local dimensionality of the spatial distribution of spin labels. The background decay, V_{inter}, is thus a function of λ and the spin concentration in the sample. Accordingly, in order to estimate the concentration of the internalized protein during hypo-osmotic swelling, DEER measurements were carried out on S20C/G35C-Gd^{3+}-DOTA-M in solution at different

dx.doi.org/10.1021/ja5079392 | J. Am. Chem. Soc. 2014, 136, 13458–13465

concentrations (ranging from 25 to 150 μM) under the same experimental conditions, and the extracted decay values from each DEER trace were used for building a calibration curve. A plot of the extracted decay rates versus concentration is shown in Figure 4a. Another calibration curve based on the maximum intensity of the ED EPR spectrum is shown in Figure 4b. Here, due to the signal intensity dependence of the echo decay rate, which is concentration dependent, the signal intensity was corrected by extrapolation to zero time. After linear regression of both data sets, the location of the *in-cell* data points on these curves should yield the local concentration in the cell for the DEER measurements and the bulk concentration for the echo intensity measurements. While the signal intensity gave a "bulk" concentration of ~4.5 μM, the DEER data gave a significantly higher local concentration of ~110 μM. The implications of these numbers will be discussed later. The *in-cell* bulk and local concentrations of the protein obtained under different cell delivery conditions are given in Table S1.

Fluorescence Measurements. The intracellular compartmentalization of the probe inside the cells following hypo-osmotic swelling was confirmed by confocal fluorescence microscopy. In this case, S20C/G35C ubiquitin was labeled with ATTO488-maleimide (ATTO488-M), and the hypo-osmotic swelling was reproduced under exactly the same conditions employed for DEER measurements. Some representative images showing a homogeneous spreading of the protein inside the cellular cytoplasm are shown in Figure 5.

Figure 5 describes the uptake of S20C/G35C-ATTO488-M immediately after the hypo-osmotic shock (1 h after returning to physiological osmolarity) (Figure 5A–C), 3 h (Figure 5D–F), and 18 h (Figure 5G–I). The fluorescence signal is exclusively associated with the cells, and no signal was detected in the background. Fluorescence signal was found in all cells, and both diffuse fluorescence and distinct fluorescence dots were observed within the cells immediately after osmotic shock. At longer times, most of the fluorescence was detected as discrete and intense spots. This experiment also demonstrated the viability of the cells upon osmotic shock, as adhesion and cell growth occurred when the cells were seeded again in the media.

While these results show that the protein is indeed internalized in the cells, they also show that it is both situated in the cytoplasm, as evident from the more uniform spread of the fluorescence in some cells (Figure 5A–C, D–F), and probably in endosomes due to the presence of intense spots. Interestingly, the localization in endosomes seems to develop with time (Figure 5G–I). After 18 h the intense spots seem to be located in certain regions of the cells suggesting either aggregation of ubiquitin and/or subcellular localization in the endoplasmic reticulum (see additional pictures in the Supporting Information). The DEER measurements were carried out on frozen samples at times where ubiquitin did not undergo through a redistribution process and it is seems to be localized both in the cytoplasm and in endosomes. The different distribution of the protein inside the cells can be explained considering the different time exposure to the solvent and the different stage of the cellular cycle of each cell. A similar inhomogeneity in the intracellular distribution was also observed for some cell penetrating peptides.[31,32] A recent *in-cell* NMR study reported that yeast growth on dextrose packs ubiquitin into protein storage bodies.[33]

DISCUSSION

The results presented here show that the distance distributions within a spin labeled protein localized inside human cells can be determined using DEER. This was achieved owing to combination of the following factors: (i) choice of novel Gd^{3+}-based spin labels and protein linkers that are stable under *in-cell* conditions; (ii) high-field measurements that feature high sensitivity for Gd^{3+}, thus allowing the detection of low concentrations and use of small sample sizes; (iii) efficient delivery of the labeled protein into the cells reaching *in-cell* concentrations sufficient for carrying out DEER measurements while maintaining cell viability; and (iv) obtaining long echo decays through D_2O exchange.

The efficiency of Gd^{3+} chelates, particularly DOTA derivatives, as a spin labels for *in vitro* DEER measurements has already been demonstrated.[34] Such measurements have been reported for peptides in solutions and membranes[35,36] and proteins[26,37] with high absolute sensitivity (~0.15 nmol) reaching distances as long as 6 nm. The EPR spectroscopic properties of high-spin Gd^{3+} ($S = 7/2$) offers a number of critical advantages for high-field EPR distance measurements. Its spin is closely localized on the Gd^{3+} atom, and its zero field splitting (ZFS) parameter, D, is relatively small in most complexes ($D < 40$ mT).[38] Consequently, the width of the subspectrum of the central $|-1/2> \rightarrow |1/2>$ transition is narrow for spectrometer frequencies (ν_0) higher than 30 GHz because it is proportional to D^2/ν_0. This is the reason for the high sensitivity. It also allows for efficient signal averaging due to its relatively short spin–lattice relaxation. As Gd^{3+} chelates are routinely used as MRI contrast agents in medicine, they may represent the candidate of choice for in *in-cell* DEER provided that the appropriate instrumentation is available. This is very important because the choice of the delivery method is not limited by the lifetime of the label as the intracellular signal exists over a considerable period of time. This is an important feature for following changes in the *in-cell* conformation of a protein upon an external stimulus or upon delivery of a second partner protein.

Protein entrapment into cells represents a difficult challenge, and several techniques for the introduction of biomolecules into cells have been explored.[12,14,39,40] Hypotonic swelling has so far been demonstrated as an efficient and biocompatible method for labeling cells with small molecules such as Gd^{3+} contrast agents.[23,24,41] We have shown that by increasing the osmotic pressure (90–100 mOsm) it is also possible to introduce small proteins such as ubiquitin (8.5 kDa) into the cell. Operational simplicity, time efficiency, and high probability of cellular viability are the main advantages of this technique.

The extracted distance distribution (Figure 3c) obtained from *in-cell* DEER trace is similar to that obtained from the *in vitro* experiment suggesting ubiquitin takes similar structures in *in-cell* and *in vitro* environments. This interspin distance distribution is in good agreement with previous *in vitro* X-band DEER measurements on S20C/G35C labeled with conventional nitroxide spin labels.[18,42] In contrast, significant differences were observed in the background decay, which is substantially stronger *in-cell* and indicates a higher local concentration. Analysis of the background decay gave a local concentration of 110 μM. This value exceeds considerably the bulk concentration of the *in-cell* samples (4.5 μM) and is larger than that used in hypo-osmotic shock, 100 μM, suggesting

dx.doi.org/10.1021/ja5079392 | J. Am. Chem. Soc. 2014, 136, 13458–13465

localization and inhomogeneous distribution in the cell, in agreement with the fluorescence measurements.

This *in-cell* bulk concentration, 4.5 μM, is actually a lower limit for the average *in-cell* concentration. In practice it is higher because the cells, although packed, do not comprise 100% of the sample and the surrounding solution does not contain any protein. Assuming that the pellet consists of about 40% of the solvent an average cell concentration of ~7.5 μM is obtained. This concentration is within the range of biologically relevant concentration of ubiquitin, considering that in HEK293 cells the total ubiquitin pool was reported to be around 80 μM.[43]

The *in-cell* detection of globular proteins like ubiquitin by NMR has been controversial both in prokaryotic and eukaryotic cells, leading to a variety of different results.[10,44] For example ubiquitin could not be observed in *E. coli*, while other proteins of comparable sizes could.[45] In this work it was concluded that transient interactions with cytoplasmic components affect the mobility of proteins, and therefore their NMR signals broaden significantly and become difficult to observe. Moreover, ubiquitin performs numerous biological functions and many of these involve interactions with other cellular proteins that can lead to broadening of the signal.[39] It was also suggested that the increased viscosity in cells is one of the main reasons for the inability to detect globular proteins. High viscosity causes the nuclei to relax quickly, thereby decreasing their detectability.[46] *In-cell* DEER as presented here is to a large extent insensitive to such processes. Therefore, once the labeled protein is introduced into the cell, DEER on Gd^{3+} is expected to be quite robust to protein size and can be a good alternative for the observation of globular proteins in cells. In principle, it should be sensitive to conformational changes upon interactions with specific partners. It is well-known that ubiquitin is present in different forms inside the cells,[43] under our experimental conditions we were not able to detect polymerization. For such a purpose singly labeled ubiquitin molecules should be used.

Based on the quality of our results we estimate that DEER measurements on *in-cell* bulk concentrations lower than 5 μM should be feasible in the future with either instrumental or sample improvement and compromise in SNR. This brings the concentrations accessible by our approach close to physiologically relevant concentrations. In mammalian cells the total protein concentrations have been determined to be between 50 and 250g/L, which vary with the cell types.[47−49] Many abundant proteins, that comprises 25% of the proteome in HeLa cells, such as pyruvate kinase and Hsp60, can have concentrations ranging from 5 to 15 μM and from 15 to 45 μM, respectively,[50] well within the range of sensitivity that can be reached by *in-cell* Gd^{3+} DEER. Working at low concentration is also important as it will allow detecting structural changes due to interaction with other proteins in the cell, otherwise the excess amounts of the labeled protein will mask interactions with proteins with cellular concentration.

CONCLUSIONS AND OUTLOOK

We have demonstrated that DEER on Gd^{3+}-DOTA-M labeled proteins can be used for structural studies of proteins inside human cells with an *in-cell* concentration lower than 10 μM. In addition it can provide the local concentration within the cell, which in turn gives indirect information regarding localization. Our new approach features chemical stability, high sensitivity, and small operational volume, which are essential for efficient *in-cell* DEER. We showed that, within the experimental accuracy of the method, the conformation of monomeric ubiquitin in Hela cells is the same as in very dilute solutions (25 μM). This indicates that its conformation is not affected by the molecular crowding in the cell. While the DEER measurements presented here were carried on a home-built W-band EPR spectrometer, Q-band measurements can also be efficient, although with some reduction in absolute sensitivity.[27] Commercial Q-band pulse EPR spectrometers are currently more abundant than W-band spectrometers.

The *in-cell* stability of the Gd^{3+} labels allowed the introduction of a simple protein delivery method that overcomes the limitation imposed by the use of oocytes and microinjection. It can be easily extended to other eukaryotic cells lines, thus allowing comparative studies. The prospect of carrying out structural studies of proteins with *in-cell* concentrations of only a few μM is exciting and opens new opportunities for watching biomolecules inside the cell, for example, exploring the effects of crowding and confinement on protein structure, probing conformational changes due to interaction with other cell components; in this context the intracellular behavior of intrinsically disordered proteins should be particularly interesting. Another interesting potential application would be deciphering the early stages of aggregation processes of proteins involved in Alzheimer and Parkinson deceases. As these measurements are carried out on frozen cells they provide a snapshot of the structure at the moment of freezing and can be used to follow a time course of a process. Combination with florescence microscopy, as shown in this work, can be used to correlate structural features with cell localization.

To further expand the applicability of this *in-cell* DEER approach the limitation of the delivery method in terms of molecular size has to be evaluated, and Gd^{3+} tags with more rigid tethers should be developed. Finally, the presented approach should be expanded to include nucleic acids.

EXPERIMENTAL SECTION

Protein Preparation. Two mutations, S20C and G35C, were introduced into the human ubiquitin gene, which was subsequently cloned into pET21a (resulting in a plasmid encoding an N-terminal 6xHis-ubiquitin fusion). *E. coli* BL21(DE3) cells transfected with the plasmid were grown in 5 L LB medium at 37 °C until mid log phase, and protein expression was induced by the addition of 0.2 mM IPTG overnight at 15 °C. Bacteria were harvested by centrifugation, and the pellet was resuspended in 100 mL lysis buffer (50 mM Tris pH 7.5, 500 mM NaCl, 20 mM imidazole, 5 mM β-mercaptoethanol (BME), 100 μL protease inhibitor cocktail set III (Calbiochem), 100 μg DNase, 1 mM PMSF, and lysozyme (4000 units)) and lysed by a cell disruptor. The insoluble material was removed by centrifugation at 26,000 *g* for 30 min. The supernatant was filtered and loaded onto a Ni column (HiTrap_chelating_HP, GE) equilibrated with buffer (50 mM Tris pH 7.5, 500 mM NaCl, 20 mM imidazole, 5 mM BME). The protein was eluted in one step with the same buffer containing 0.5 M imidazole. Fractions containing the fusion protein were loaded onto a size exclusion column (HiLoad_16/60_Superdex 75, GE) and equilibrated with buffer containing 50 mM Tris pH 7.5, 200 mM NaCl, and 5 mM BME. Pure ubiquitin fractions were determined by SDS-PAGE and combined.

Protein Labeling. DOTA-M tag was used because the maleimide function attaches the spin label to the cysteine residues through a C−S bond which is stable in the cell environment.[51] Gd^{3+}-DOTA-M was prepared by dissolving 1 mol of maleimide-monoamino-DOTA (Macrocyclics, Inc.) and 1.1 mol of $GdCl_3$ (Sigma-Aldrich) in distilled water and stirring at room temperature for 3 h. NaOH was slowly added to bring the pH to approximately 5.5−6. After 3 h the mixture was freeze-dried to get a white powder.

dx.doi.org/10.1021/ja5079392 | J. Am. Chem. Soc. 2014, 136, 13458−13465

Before labeling the protein, BME (used as stabilizer) was removed from the protein solution. Thus, a S20C/G35C His-Ub solution (6.3 mg/mL) was passed through a PD-10 desalting column in 20 mM potassium phosphate buffer (pH 6.8) containing 5 mM KCl. The eluate was directly added to a 20-fold molar excess Gd^{3+}-DOTA-M solution (300 μL) in anhydrous DMF. The PD-10 running buffer was 20 mM potassium phosphate buffer (pH 6.8) containing 5 mM KCl. The mixture was incubated at room temperature for 4 h under inert atmosphere to prevent oxidation of thiols. Unreacted spin label was removed by size exclusion chromatography (HiLoad 16/60 Superdex 30) by using 20 mM potassium phosphate buffer pH 6.8 containing KCl 5 mM as mobile phase.

The same procedure was followed for labeling the protein with ATTO488-maleimide (ATTO488-M) (ATTO-Tech) except that it exceeded the protein concentration by 2-fold.

Growth of HeLa Cells. HeLa cells were grown in DMEM media (GIBCO, Invitrogen) supplemented with 10% bovine serum (GIBCO, Invitrogen), 5 mM L-glutamin (Biological Industries), and penicillin-streptomicyn (Biological Industries) at 37 °C with 5% of CO_2. Cells were diluted from 80% − 100% confluency to about 20% confluency every 48 h using trypsin-EDTA (Biological Industries).

Loading of S20C/G35C-Gd^{3+}-DOTA-M and S20C/G35C-ATTO488-M by Hypotonic Swelling. The intracellular delivery of S20C/G35C-Gd^{3+}-DOTA-M and S20C/G35C-ATTO488-M has been carried out by means of the hypotonic swelling procedure that has been shown to be particulary efficient in cell labeling with Gd^{3+}-chelates.[41] HeLa cells were suspended in 200 μL of a hypotonic solution (90−100 mOsm) containing either 0.1 mM S20C/G35C-Gd^{3+}-DOTA-M or 0.1 mM S20C/G35C-ATTO488-M (PBS solution was used to reach the final osmolarity) and incubated at 37 °C for 60 min. Then the osmolarity of the external solution was restored to an isotonic condition (280 mOsm) through the addition of a proper concentration of phosphate buffer saline and maintained for another 60 min at 37 °C. The osmolarity of the solutions was monitored with a Vitech Scientific 3300 Advanced Micro Osmometer. After treatment, the cells were extensively washed with PBS in D_2O to remove the noninternalized protein and then incubated at 37 °C for 15 min using the same PBS buffer in D_2O (simply PBS for S20C/G35C-ATTO488-M). The cells were incubated for an additional 10 min and washed twice with a solution containing PBS in D_2O and d_8-glycerol (8/2 v/v). Finally, the cells were loaded into an EPR quartz capillary (0.6 ID × 0.84 OD mm) and centrifuged to create a pellet, and then the capillary was slowly frozen in an isopropanol rack at −80 °C. To check for residual protein in solution, the echo detected EPR spectra of the buffer used for the last wash was acquired, and no signal was found.

Other conditions with different protein concentrations and osmotic pressures were also explored in order to optimize the loading efficiency during hypotonic swelling procedure (see Figure S1).

EPR Measurements. All measurements were carried out on a home-built W-band spectrometer.[52] W-band ED EPR spectra were recorded at 10 K using $\pi/2$ and π pulse durations of 30 and 60 ns, respectively, with an echo delay of 750 ns and a repetition time of 1 ms.

Echo decays were measured by Hahn echo decay experiments ($\pi/2$-τ-π-τ-echo) at the DEER observer frequency (see below) (Figure 2). The $\pi/2$ and π pulse durations were 15 and 30 ns, respectively. The measurements were performed at 10 K with a repetition time of 750 μs and two-step phase cycling.

DEER measurements were carried out at 10 K using the standard four-pulse DEER sequence (Figure 1c). The pump pulse duration was 15 ns, and the observer pulses were 15 and 30 ns, respectively. The frequency difference between the pump and observer pulses was 90 MHz, with the pump pulse set to the maximum of the EPR spectrum as shown in Figure 2a. This setup was chosen because it represents a good compromise between modulation depth, λ, and phase memory time, T_M. Even though the echo intensity is maximized by setting the observer pulse in the central transition, this setup requires very high stability of the spectrometer and high dynamic range because a small change is observed for a very large signal.[34]

The repetition delay was 800 μs, and accumulation times were about 1.5 h for *in vitro* measurements and about 18 h for the *in-cell* samples. An eight-step phase cycle was employed: $\pi/2_{obs}$: $+x, -x, +x, -x, +x, -x, +x, -x$; π_{obs}: $+x, +x, +x, +x, -x, -x, -x, -x$; π_{pump}: $+x, +x, -x, -x, +x, +x, -x, -x$; π_{obs}: $+x, +x, +x +x, +x, +x, +x, +x$. The receiver phase cycle was +, −, +, −, +, −, +, −. The phase cycling was needed to remove instrumental artifacts and to compensate for DC offset.

The DEER data were analyzed using the program DeerAnalysis 2011.[30] Distance distributions were obtained using Tikhonov regularization with a regularization parameter of 1000. SNR of DEER traces were calculated taking into account 3 times the standard deviation (3σ) of the data at the end of the trace.

Confocal Fluorescence Microscopy. HeLa cellular labeling with S20C/G35C-ATTO 488-M was carried out by means of the same hypo-osmotic shock procedure for S20C/G35C-Gd^{3+}-DOTA-M, except that simple PBS buffer (no D_2O) was used for washing. Cells were imaged in PBS immediately after the treatment and plated into 12 mm glass-bottomed dishes and cultured for 24 h.

A sealed chamber was built for live imaging using microscope glass slides, Parafilm, and double side tape in a sandwich configuration. A rectangular strip (18 × 25 mm) of double-sided tape was glued on a sandblasted single frosted precleaned microscope glass slide (ThemoScientific) 25 × 75 × 1 mm thick. A rectangular strip of Parafilm (20 × 30 mm) was then glued over the upper side of the double layer tape. A second strip of double side tape (18 × 25 mm) was thus glued over the Parafilm layer. Finally a second strip of Parafilm (20 × 30 mm) was then glued over the upper side of the double layer tape. A chamber of 12 × 12 mm was cut through the tape/Parafilm layers by using a razor blade. The bottom down glass in the chamber was cleaned using 70% ethanol in order to remove residuals of glue. The volume of the chamber was about 100 μL. The chamber was sealed using high-precision microscope cover glasses 22 × 22 mm, 170 ± 5 μm, no. 1.5H (Marienfield-Superior).

Cells were imaged in PBS immediately after the treatment by transferring 100 μL of cell suspension to the imaging chamber and sealing it with the microscope cover glass (Marienfield-Superior).

Alternatively, cells were centrifuged for 3 min at 220 *g* (1300 rpm) in a Apogee Swing-3000 horizontal centrifuge, resuspended in the complete growth media, and plated in 100 × 20 mm cell culture dishes (BD Biosciences) containing microscope cover glasses (Marienfield-Superior) previously treated with 300 μL of 20 μg/μL fibronectin from bovine plasma (Sigma-Aldrich) in PBS buffer for 45 min at 37 °C. HeLa cells adherent to the microscope cover glass were then imaged 3 or 24 h after plating by washing the microscope cover glass in PBS and sealing the imaging chamber containing 100 μL of PBS with the side of the cells facing down. Distribution of S20C/G35C-ATTO488-M was analyzed in living HeLa cells using a confocal laser-scanning microscope (Olympus Fluoview 300) equipped with a PlanApo 60×/N.A. 1.20 water immersion objective. The fluorescence signal was detected by excitation with the 488 nm argon laser (Mellet Griot) using an emission filter (510−530 nm).

■ ASSOCIATED CONTENT

Supporting Information

Optimization of the protein delivery procedure and associated DEER data and additional confocal microscopy pictures of the cells with fluorescent labeled ubiquitin. This material is available free of charge via the Internet at http://pubs.acs.org.

■ AUTHOR INFORMATION

Corresponding Author

Daniella.Goldfarb@weizmann.ac.il

Notes

The authors declare no competing financial interest.

■ ACKNOWLEDGMENTS

This research was supported by the F.I.R.S.T. program of the Israel Science Foundation (ISF, grant number 1114/12) and the De Benedetti Foundation Cherasco. We thank Prof. Michael Elbaum for helpful discussions and for letting us use his confocal microscope, Prof. Menahem Segal and Dr. Eduard Korkotian for making their osmometer available to us, Drs. Shira Albeck and Tami Unger from the Proteomics unit at the Weizmann Institute for the preparation of the ubiquitin mutant, and Dr. Yoav Barak for helping with the protein purification. We thank Prof. Michal Neeman and her team for their advice and support in the early stages of the project. This research was also made possible in part by the historic generosity of the Harold Perlman Family. D.G. holds the Erich Klieger Professorial Chair in Chemical Physics.

■ REFERENCES

(1) Mayor, S.; Bilgrami, S. *Fretting about FRET in cell and structural biology in "Evaluating Techniques in Biochemical Research*; D. Zuk; Cell Press: Cambridge, 2007; pp 43−49.
(2) Singh, D. R.; Mohammad, M. M.; Patowary, S.; Stoneman, M. R.; Oliver, J. a; Movileanu, L.; Raicu, V. *Integr. Biol.* **2013**, *5*, 312.
(3) Albizu, L.; Cottet, M.; Kralikova, M.; Stoev, S.; Seyer, R.; Brabet, I.; Roux, T.; Bazin, H.; Bourrier, E.; Lamarque, L.; Breton, C.; Rives, M.-L.; Newman, A.; Javitch, J.; Trinquet, E.; Manning, M.; Pin, J.-P.; Mouillac, B.; Durroux, T. *Nat. Chem. Biol.* **2010**, *6*, 587.
(4) Fessl, T.; Adamec, F.; Polívka, T.; Foldynová-Trantírková, S.; Vácha, F.; Trantírek, L. *Nucleic Acids Res.* **2012**, *40*, e121.
(5) Parsons, M.; Vojnovic, B.; Ameer-Beg, S. *Biochem. Soc. Trans.* **2004**, *32*, 431.
(6) An, S. J.; Almers, W. *Science* **2004**, *306*, 1042.
(7) Carriba, P.; Navarro, G.; Ciruela, F.; Ferré, S. *Nat. Methods* **2008**, *5*, 727.
(8) Llères, D.; James, J.; Swift, S.; Norman, D. G.; Lamond, A. I. *J. Cell Biol.* **2009**, *187*, 481.
(9) Freedberg, D.; Selenko, P. *Annu. Rev. Biophys.* **2014**, *43*, 171−192.
(10) Sakai, T.; Tochio, H.; Tenno, T.; Ito, Y.; Kokubo, T.; Hiroaki, H.; Shirakawa, M. *J. Biomol. NMR* **2006**, *36*, 179.
(11) Ogino, S.; Kubo, S.; Umemoto, R.; Huang, S.; Nishida, N.; Shimada, I. *J. Am. Chem. Soc.* **2009**, *131*, 10834.
(12) Danielsson, J.; Inomata, K.; Murayama, S.; Tochio, H.; Lang, L.; Shirakawa, M.; Oliveberg, M. *J. Am. Chem. Soc.* **2013**, *135*, 10266.
(13) Selenko, P.; Serber, Z.; Gadea, B.; Ruderman, J.; Wagner, G. *Proc. Natl. Acad. Sci. U. S. A.* **2006**, *103*, 11904.
(14) Banci, L.; Barbieri, L.; Bertini, I.; Luchinat, E.; Secci, E.; Zhao, Y.; Aricescu, a R. *Nat. Chem. Biol.* **2013**, *9*, 297.
(15) Kubo, S.; Nishida, N.; Udagawa, Y.; Takarada, O.; Ogino, S.; Shimada, I. *Angew. Chem., Int. Ed. Engl.* **2013**, *52*, 1208.
(16) Milov, A. D.; Ponomarev, A. B.; Tsvetkov, Y. D. *Chem. Phys. Lett.* **1984**, *110*, 67.
(17) Pannier, M.; Veit, S.; Godt, a; Jeschke, G.; Spiess, H. W. *J. Magn. Reson.* **2000**, *142*, 331.
(18) Igarashi, R.; Sakai, T.; Hara, H.; Tenno, T.; Tanaka, T.; Tochio, H.; Shirakawa, M. *J. Am. Chem. Soc.* **2010**, *132*, 8228.
(19) Krstić, I.; Hänsel, R.; Romainczyk, O.; Engels, J. W.; Dötsch, V.; Prisner, T. F. *Angew. Chem., Int. Ed. Engl.* **2011**, *50*, 5070.
(20) Holder, I. T.; Drescher, M.; Hartig, J. S. *Bioorg. Med. Chem.* **2013**, *21*, 6156.
(21) Azarkh, M.; Singh, V.; Okle, O.; Dietrich, D. R.; Hartig, J. S.; Drescher, M. *ChemPhysChem* **2012**, *13*, 1444.
(22) Thonon, D.; Jacques, V.; Desreux, J. F. *Contrast Media Mol. Imaging* **2007**, *34*, 24.
(23) Rossi, L.; Serafini, S.; Pierigé, F.; Antonelli, A.; Cerasi, A.; Fraternale, A.; Chiarantini, L.; Magnani, M. *Expert Opin. Drug Delivery* **2005**, *2*, 311.
(24) Markov, D. E.; Boeve, H.; Gleich, B.; Borgert, J.; Antonelli, a; Sfara, C.; Magnani, M. *Phys. Med. Biol.* **2010**, *55*, 6461.
(25) Raitsimring, A. M.; Gunanathan, C.; Potapov, A.; Efremenko, I.; Martin, J. M. L.; Milstein, D.; Goldfarb, D. *J. Am. Chem. Soc.* **2007**, *129*, 14138.
(26) Potapov, A.; Yagi, H.; Huber, T.; Jergic, S.; Dixon, N. E.; Otting, G.; Goldfarb, D. *J. Am. Chem. Soc.* **2010**, *132*, 9040.
(27) Raitsimring, a; Astashkin, a V; Enemark, J. H.; Kaminker, I.; Goldfarb, D.; Walter, E. D.; Song, Y.; Meade, T. *J. Appl. Magn. Reson.* **2013**, *44*, 649.
(28) Jeschke, G.; Polyhach, Y. *Phys. Chem. Chem. Phys.* **2007**, *9*, 1895.
(29) Siegel, B. V.; Lund, R. O.; Wellings, S. R.; Bostic, W. L. *Exp. Cell Res.* **1959**, *19*, 187.
(30) Jeschke, G.; Chechik, V.; Ionita, A.; Godt, A.; Zimmermann, H.; Banham, J.; Timmel, C. R.; Hilger, D.; Jung, H. *Appl. Magn. Reson.* **2006**, *30*, 473.
(31) Guterstam, P.; Madani, F.; Hirose, H.; Takeuchi, T.; Futaki, S.; El Andaloussi, S.; Gräslund, A.; Langel, U. *Biochim. Biophys. Acta* **2009**, *1788*, 2509.
(32) Duchardt, F.; Fotin-Mleczek, M.; Schwarz, H.; Fischer, R.; Brock, R. *Traffic* **2007**, *8*, 848.
(33) Bertrand, K.; Reverdatto, S.; Burz, D. S.; Zitomer, R.; Shekhtman, A. *J. Am. Chem. Soc.* **2012**, 12798.
(34) Goldfarb, D. *Phys. Chem. Chem. Phys.* **2014**, *16*, 9685.
(35) Gordon-Grossman, M.; Kaminker, I.; Gofman, Y.; Shai, Y.; Goldfarb, D. *Phys. Chem. Chem. Phys.* **2011**, *13*, 10771.
(36) Matalon, E.; Huber, T.; Hagelueken, G.; Graham, B.; Frydman, V.; Feintuch, A.; Otting, G.; Goldfarb, D. *Angew. Chem., Int. Ed. Engl.* **2013**, *52*, 11831.
(37) Yagi, H.; Banerjee, D.; Graham, B.; Huber, T.; Goldfarb, D.; Otting, G. *J. Am. Chem. Soc.* **2011**, *133*, 10418.
(38) Raitsimring, A. M.; Astashkin, A. V.; Poluektov, O. G.; Caravan, P. *Appl. Magn. Reson.* **2005**, *28*, 281.
(39) Sakai, T.; Tochio, H.; Tenno, T.; Ito, Y.; Kokubo, T.; Hiroaki, H.; Shirakawa, M. *J. Biomol. NMR* **2006**, *36*, 179.
(40) Ogino, S.; Kubo, S.; Umemoto, R.; Huang, S.; Nishida, N.; Shimada, I. *J. Am. Chem. Soc.* **2009**, *131*, 10834.
(41) Di Gregorio, E.; Ferrauto, G.; Gianolio, E.; Aime, S. *Contrast Media Mol. Imaging* **2013**, *8*, 475.
(42) Hara, H.; Tenno, T.; Shirakawa, M. *J. Magn. Reson.* **2007**, *184*, 78.
(43) Kaiser, E. S.; Riley, E. B.; Shaler, A. T.; Trevino, S. R.; Becker, H. C.; Schulman, H.; Kopito, R. R. *Nat. Methods* **2011**, *8*, 691.
(44) Barnes, C. O.; Monteith, W. B.; Pielak, G. J. *ChemBioChem* **2011**, *12*, 390.
(45) Wang, Q.; Zhuravleva, A.; Gierasch, M. L. *Biochemistry* **2012**, *50*, 9225.
(46) Li, C.; Charlton, L. M.; Lakkavaram, A.; Seagle, C.; Wang, G.; Young, G. B.; Macdonald, J. M.; Pielak, G. J. *J. Am. Chem. Soc.* **2008**, *130*, 6310.
(47) Cheung, M. C.; LaCroix, R.; McKenna, B. K.; Liu, L.; Winkelman, J.; Ehrlich, D. J. *Cytometry, Part A* **2013**, *83*, 540.
(48) Conlon, I.; Raff, M. *J. Biol.* **2003**, *2*, 1.
(49) Zeskind, B. J.; Jordan, C. D.; Timp, W.; Trapani, L.; Waller, G.; Horodincu, V.; Ehrlich, D. J.; Matsudaira, P. *Nat. Methods* **2007**, *4*, 567.
(50) Nagaraj, N.; Wisniewski, J. R.; Geiger, T.; Cox, J.; Kircher, M.; Kelso, J.; Pääbo, S.; Mann, M. *Mol. Syst. Biol.* **2011**, *7*, 548.
(51) DeForest, C. A.; Polizzotti, B. D.; Anseth, K. S. *Nat. Mater.* **2009**, *8*, 659.
(52) Goldfarb, D.; Lipkin, Y.; Potapov, A.; Gorodetsky, Y.; Epel, B.; Raitsimring, A. M.; Radoul, M.; Kaminker, I. *J. Magn. Reson.* **2008**, *194*, 8.